Original Paper

Determination of stoichiometry from polycrystalline powders of transition metals lamellar dichalcogenides: MoSe$_2$, WSe$_2$, obtained by synthesis in laboratory

Jacques SAWADOGO[1,4*], Moussa BOUGOUMA[1,2], Jean Boukari LEGMA[1] and Marie–Paule Delplancke OGLETREE[3]

[1]*Laboratoire de Chimie Moléculaire et des Matériaux Equipe Chimie Physique et d'Electrochimie, UFR/SEA, Université de Ouagadougou 03 BP 7021 Ouagadougou 03, Burkina Faso.*
[2]*Faculté des Sciences, Services de Chimie Analytique et Chimie des Interfaces (CHANI) Université Libre de Bruxelles Campus de la Plaine Boulevard du Triomphe CP 255 B-1050, Bruxelles, Belgique.*
[3]*Service Matières et Matériaux, Groupe Chimie Industrielle, Faculté des Sciences Appliquées, Université Libre de Bruxelles CP 165/63, Avenue F.D.Roosevelt 50 B-1050 Bruxelles, Belgique.*
[4]*Institut de l'Environnement et de Recherches Agricoles (INERA), Département Gestion des Ressources Naturelles et des Systèmes de Productions, Laboratoire Sol-Eau-Plantes, 04 BP 8645 Ouagadougou 04, Burkina Faso, Tél. : 00226 25 34 02 70; Fax. : 00226 25 34 02 71.*
[*]*Corresponding author; E-mail: jacquischimie@gmail.com; jacquischimie@hotmail.fr; Tel: (+226) 78 28 40 66/ (+226) 78 82 42 46*

ABSTRACT

Polycrystalline molybdenum and tungsten (MoSe$_2$, WSe$_2$) diselenides were synthesized at 1323 K for 168 hours in silica tubes sealed secondary vacuum. They were characterized by diffraction with X-Ray diffraction (XRD), Scanning Electron Microscopy (SEM) and gravimetric analysis show that they are homogeneous and well crystallized. Electrochemical and chemical dosages were used to determine their stoichiometry. The results have shown that stoichiometry is reached only when using B type powders and a difference in layer piling according to the mode of synthesis; this explains why A type powders differ from B type powders due to the piling of 2H: 3R layers.
© 2015 International Formulae Group. All rights reserved.

Keywords: Polycrystalline powders, MoSe$_2$, WSe$_2$, SEM, X-Ray diffraction, gravimetry and electrochemical.

INTRODUCTION

Molybdenum diselenide (MoSe$_2$) and tungsten diselenide (WSe$_2$) are transition metal semiconducting dichalocogenides, which crystallize in the 2H-MoS$_2$ structures. The 2Hb- polytype of these MSe$_2$ (M = Mo, W) layer compounds consists of three planes: one hexagonal plane consisting of the metal ions M, placed between two hexagonal planes consisting of the Se ions (Vollath et al., 2006). Over these last years, the almost short or long term depletion of fossil energies sources such as gas and oil has boosted researches in the area of substitution energies, particularly the conversion of solar energy into electric energy. Previous works conducted in this

laboratory (Forker et al., 2000; Vollath et al., 2006) have first allowed to characterize and second to clarify the conditions for improving the photocurrent gain and consequently, the conversion efficiency of $MoSe_2$ and WSe_2 photo electrode. In the literature (Liu et al., 2011; Radisavljevic et al., 2011), the stoichiometry of polycrystalline powders used in vapor transport to obtain single crystals has a significant impact on the quality of crystals. Thus, to obtain crystals with few surface defects and which can be connected in the electrode in electrochemical cells, the stoichiometry of these polycrystalline powders should be well controlled (Bougouma et al., 2008; Perkin et al., 2013; Zhu et al., 2013). This requires the use of accurate methods of chemical and electrochemical analyzes to determine major elements of semiconductor materials synthesized in the laboratory, in order to clarify the stoichiometry. Characterizations of these materials with X-ray diffraction (XRD) and Scanning Electron Microscopy (SEM) were also performed.

The objective of this work was to show that the variation of synthesis conditions of $MoSe_2$ and WSe_2 polycrystalline powders impacts on the stoichiometry, and how this stoichiometry gap can be correlated to the structure and morphology of these powders. In order to improve conditions for the synthesis of semiconductor materials ($MoSe_2$ and WSe_2 polycrystalline powders and single crystals), a sound knowledge of the following factors is mandatory: stoichiometry, texture and surface structure of the crystalline material. This work is a contribution to improve synthesis conditions for lamellar dichalcogenides of MSe_2 (M = Mo, W) transition metals.

MATERIALS AND METHODS
Synthesis of MSe_2 (M= Mo, W) powder diselenides

The synthesis of $MoSe_2$ and WSe_2 Polycrystalline powders from known purity elements is done by using a simple equation (1):

$$M \;+\; 2X \longrightarrow MX_2$$

Where M represents the molybdenum or tungsten and X the metallic selenium. The syntheses were in silica glass tubes sealed under secondary vacuum (10^{-6} Torr or $13.32.10^{-5}$ Pa) (Figure 1). For the synthesis of molybdenum and tungsten diselenides, the ampoule contained a mixture of molybdenum or tungsten powder, Koch-Light, 99.9% pure; and granular selenium, Koch-Light, 99.999% pure. The overall quantity of product does not exceed five (5) grams due to the high heat pressure of components. The synthesis is done in 8 mm large and 120 mm length silica tube. This reaction chamber is prior degreased with detergent, then rinsed several times with distilled water and alcohol. Lastly, it is dried in an incubator for at least 24 hours at 383 K. Once the high vacuum is reached, tubes are sealed with torch. They are then introduced into the synthesis furnace (Figure 2) characterized by an area without thermal gradient. The temperature is raised at the end of 48 hours, to synthesize temperature (Ts) of between 873 and 1023 K, by successive bearings. This bearing allows to avoid a very high overpressure within the bulb by the total vaporization of the chalcogen beyond its boiling point (T_{vap} = 958 K for selenium). The synthesis is achieved by maintaining this temperature for five (5) to seven (7) days, and the product of the synthesis is cooled in two ways:

- The first consists in cooling the synthesis tube within the furnace for half a day (12 hours), A type powders;
- The second consists in an air quench, i.e. to withdraw the synthesis tube for the furnace and let it cool down in open air, B type powders.

In either case, the result is a black polycrystalline powder. These powders, after grinding and selection of all residues, are once again introduced into a bulb of the same type, degassed and sealed under vacuum again. The bulb is then put under a prolonged annealing for five (5) to seven (7) days at an annealing

temperature T_R ranging between 1273 K and 1323 K. The bulbs are removed after 12 hours after full stop and cooling of the furnace. The annealing ensures better recrystallization of the polycrystalline powder which becomes very bright.

Methods

The synthesis of polycrystalline powders MSe_2 (M = Mo, W) is made using an ILMVAC and DHV200M type of vacuum pump, (Figure 1) and after sealing bulbs are inserted into a 201 CARBOLITE furnace illustrated on Figure 2. To determine the stoichiometry of the polycrystalline powders, various methods are used.

X-Ray diffraction (DRX)

This method enables to identify the nature of the various phases. The structural parameters of the polycrystalline powders were determined by X-ray powder diffraction (XRD) using a nickel-filtered Cu-Kα radiation ($\lambda = 1.5406$ Å) in a Siemens D5000 apparatus (Brüker), and the computer programs Diffrac Plus and Topaz V2.0**.** This modern diffractometer is connected with a computer equipped with the following software: Diffrac Plus and Topas, version 2.0 to calculate the parameters of the mesh (Perkins et al., 2013). This software which is appropriate for crystallographic calculations was used to calculate Miller Indexes (Tables 1a and 1b), the intensities of the diffraction spectra lines, mesh parameters and d_{hkl} reticular distances of the various samples The XRD data were recorded in the 2θ-range 10 -70° at a scan speed of 0.08° min⁻¹. Lattice parameters were refined using a least-squares technique (JCPDS X-ray Powder Data file, Pattern: 01-077-1715; JCPDS X-ray Powder Data file, Pattern: 01- 087-2418).

Scanning Electron Microscopic (SEM)

The scanning electron microscopy (SEM JEOL JSM-6100) was used for the morphological characterization of the powders.

The Se/Mo ratios of the samples $MoSe_2$ and WSe_2 were analyzed by a gravimetric, potentiometric and Conductimetric procedure (Li et al., 2011; Huang et al., 2013).

Gravimetric procedure

The stoichiometry of crystalline powders $MoSe_2$ and WSe_2 then obtained is controlled by determining the metal content of the compound using a gravimetric method. The samples were oxidized in air at 1023 K and 1123 K for 8 h giving MoO_3 and WO_3 respectively. The metal M (M = Mo, W) content of the samples was determined from the mass of MO_3 formed. The Se content was then estimated by subtraction of the metal mass from the initial mass of the sample.

Potentiometric

This consists in determining the potential of a specific electrode immersed in a solution whose concentration in electroactive substances varies (Sortais-Soulard et al., 2004). The type of potentiometer used is DIGITAL pH – meter millivoltmeter of mark MINI 80.

Conductimetric

This enables to obtain concentrations. The conductimeter used is CO 3000L of standard mark PH1000L pHenomenal®.

These electrochemical methods (potentiometric and conductimetric) required the use of working equipment like:

Working electrode

This selective electrode for ions plomb is a Radiometer Analytical type ISE25PB-9 (Figure 3).

Reference electrode or comparison electrode

It is a Radiometer Analytical type REF 251 second compartment filled with 0.1 M KNO_3, electrode whose potential is rigorously constant and known at $0.1 \leq \Delta V \leq 1$ mV or so.

Supporting electrolyte

A potassium nitrate solution (KNO_3 0.1 M) with addition solution: $Pb(NO_3)_2$.

RESULTS

Characterization with scanning electronic microscope (MEB)

Powders synthetized in laboratory were characterized using scanning electronic microscope of the Industrial Chemistry

Department of the Université Libre de Bruxelles (ULB). These include the following powders:

- A type Powders $MoSe_2$ (Figure 4a) and B type (Figure 4b);
- A type Powders WSe_2 (Figure 5a) and B type (Figure 5b).

This study is to understand some aspects of these powders microstructure, namely: the shape and external structure of grains, their size and piling up. These microstructures are presented on Figures 4 and 5. The Microscopic study of these microstructure samples always reveals the lamellar structure. We clearly notice individual crystallites limited by regular surfaces and laid out at random. These figures show well-crystallized individual crystallites with lamellar structures in the form of tabular hexagonal plaques whose average diameter ranges between 50 and 100 microns for B type powders of gray - black color and presents a characteristic metallic lustre, while A type powders are characterized by plaques of 10 to 48 microns diameters. The study of photographs shows that individual B type powder crystallites contain on their surfaces many brilliant points which are potential sources of new germination (Figures 4b and 5b). A type powders have very smooth surfaces, with few surface defects. Compared with B type powders which contain grains whose surfaces seem to contain fewer defects, A type powders have a much stronger metallic brilliance on the surface. These differences noticed (morphology) are probably due to A and B types powders cooling conditions.

Analysis by diffraction of X-Ray of powders synthetized in laboratory

Indexing was successfully performed for the various samples after honing the parameters. Honing was conducted by systematically adjusting structural parameters to obtain the best correspondence possible between measured intensities and those calculated from deduced structure models of diffraction of the WSe_2 and $MoSe_2$ spectra

which both crystallize in the hexagonal system with a group of space P 63/mmc. Diffraction spectra of the various samples are given in Figures 6 to 9. X-ray diffraction patterns of the polycrystalline B type powders (Figures 6 and 7) have thin diffraction peaks.

For $MoSe_2$, the most intense peaks noticed, due to a preferential orientation of the hexagonal plaques, are the reflection planes (00ℓ): (002), (006), and (008). Peaks (004) (103) (104) (108) and (105) of medium intensity are also noticed, peaks (100), (102) and (106) of very low intensity are also visible on $MoSe_2$ spectrum. The diffraction spectrum WSe_2 has intense diffraction peaks deriving from the reflection planes (002), (103) and (105). Peaks (006) (008) (100) (102) (104) and (105) of average intensities were noticed and peaks (004), (101) and (106) of low intensities are also visible on WSe_2 spectrum. X-ray diffraction spectra of A type polycrystalline powders (Figures 8 and 9) have the same diffraction lines as B type powders. We have not noticed any preferential orientation of the reflection planes (00ℓ) for A type powders. For powder $MoSe_2$, we have a very intense peak (103) and medium intensity peaks, namely (002) (100) (110) and (105). Unlike B type polycrystalline powders where all peaks are fine, the lines (103) and (105) are larger than all other lines of $MoSe_2$ X-ray diffraction A type powder. The WSe_2 powder X-ray diffraction gives a very intense peak (002) and medium intensity peaks: (100) (103) (006) (105) and (008). Data processing software integrated in the computer controlling the diffractometer enables the use of these spectra and data are summarized in Tables 1a for $MoSe_2$ and Table 1b for WSe_2. Mesh parameters on polycrystalline compounds were determined and compared to those provided by literature (Tables 2a and 2b). The replication of measures was tested on series of three data collections. Mesh parameters for WSe_2 and $MoSe_2$ compounds are identical to those found in literature. The comparative study of the calculated values of crystal parameters (Tables 2a and 2b) with

those of JCPDS database gives a good alignment.

The slight differences could be explained either by the uncertainties due to measurement devices or by manipulation errors. The examination of crystal parameters obtained by experimentation enables indexing materials studied ($MoSe_2$ and WSe_2) in the hexagonal system, confirming the literature. The study of the diffraction spectra also shows that polycrystalline powders synthesized in the laboratory are well crystallized; all diffraction lines are well resolved.

Gravimetric analysis

The gravimetric method was used to determine the stoichiometry of the polycrystalline powders MSe_2 (M = Mo, W) synthesized in laboratory. MO_3 oxide is obtained by the oxidation of MSe_2 material in air, according to the following equation:

$$MSe_{2(solide)} + \frac{3}{2}O_{2(gaz)} \longrightarrow MO_{3(gaz)} + 2Se_{(gaz)} \quad (2)$$
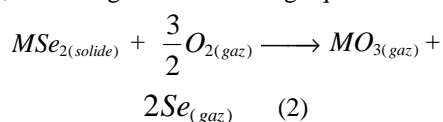
M = Mo, W

This reaction releases the chalcogen Se when it turns into gas, metal M is oxidized at a temperature T_R (1023 Kelvin for MoO_3 (white) and 1123 Kelvin for WO_3 (lemon yellow) of the chemical reaction. The whole oxide and crucible is cooled and weighed again. The resulting mass is m_2. The difference $m_2 - m_1$ is used to determine the mass of MO_3 oxide obtained, and then to calculate the metal content M (m_M) in MO_3 oxide. Se content is determined by subtracting: $m_{Se} = m_{MSe} - m_M$.

The results of gravimetric analysis of various powders are given in Table 3 and are calculated using the following formula:

$\frac{y}{x} = (\frac{m_{Se}}{m_M} . \frac{M_M}{M_{Se}})$, M_M is the molar mass of the metal, M_{Se} is the molar mass of selenium (Se). The analysis of the table shows that the Se/M_o ratio of B type polycrystalline powders is very close to the stoichiometry. However,

the ratio of A type powders differs much from the stoichiometry in the approximate range of $1.85 \leq \frac{Se}{Mo} \leq 1.9$. These differences are probably due to synthesis conditions of the various powders.

Electrochemical analysis

The dissolution of MO_3 oxide in distilled water is given by the following equation (3):

$$MO_{3(solide)} + H_2O \longrightarrow MO_4^{2-} + 2H^+ \quad (3)$$

The solution obtained is withdrawn from a Pb^{2+} solution. Titration reaction is given by the equation (4):

$$MO_4^{2-} + Pb^{2+} \longrightarrow PbMO_4 \quad (4)$$
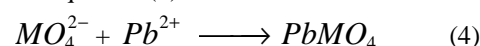
(M = W, Mo)

Since the reaction between the ion Pb^{2+} and the ion MO_4^{2-} is a reaction of an equimolar, we will have the following equivalence:

$$C_{MO_4^{2-}} = M_{MO_4^{2-}} = \frac{M_{Pb^{2+}} \times V_{Pb^{2+}}}{V_{MO_4^{2-}}} \text{ which}$$

enables first to translate the molarity of the ions MO_4^{2-} ($M = Mo, W$) into a solution, second to calculate the mass of oxides used in the dissolution. To find the total number of molars MO_4^{2-}, we use the following relation:

$$n_{MO_4^{2-}} = C_{MO_4^{2-}} \times V_{T(MO_4^{2-})}$$

Where $V_{T(MO_4^{2-})}$ is the total volume in which the oxide was dissolved, then we establish $m_{MO_3} = n_{MO_3} \times M_{m(MO_3)}$ from

$n_{MO_4^{2-}} = n_{MO_3}$ We deduce the mass of the metal M in MSe_2. The selenium content is calculated by making the difference:

$m_{Se} = m_{MSe} - m_M$ and the stoichiometry $\frac{Se}{M}$

in the MSe_2 compound is determined as described in the gravimetric method. Titration of MO_4^{2-} ions is followed by either potentiometry or conductimetry.

Conductimetric and potentiometric dosages consist in adding Pb^{2+} ions in a solution of WO_4^{2-} or MoO_4^{2-} with an unknown concentration. Ions Pb^{2+} reacts with ions MO_4^{2-} or MoO_4^{2-} ions to make the $PbWO_4$ or $PbMoO_4$ precipitate. The equivalent point is determined potentiometrically at zero intensity by plotting E (mV) = f (volume) or by conductimetry by plotting the curve γ (conductance) = f (volume).

Analysis of B type powders
Potentiometric dosage
Calibration of the selective electrode for ions plomb
For a better application of electrochemical methods in the determination of solutions obtained by dissolving MoO_3 and WO_3 oxides, it is necessary to calibrate our working electrode (specific lead electrode Pb^{2+}) to ensure reliable measurements. The calibration is made at a constant temperature of 30 ± 2 °C. This must be done by measuring the potential for the various concentrations of Pb^{2+} ions, the standard solutions which should all have the same ionic strength. Calibration results are given in Table 4.

The corresponding curve is given in Figure 10. This curve is linear, which enables to conclude that the electrode can be used to determine an unknown concentration of MO_4^{2-} ions in this concentration (10^{-6} M to 10^{-2} M).

Dosage of molybdates and tungstates solutions obtained by the dissolution of MO_3 (M = Mo, W)
Potentiometric dosages curves of molybdates and tungstates solutions presented in Figures 11 and 12 comprise three parts:
A linear part *c*orresponds to a substantial amount of MO_4^{2-} ions (M = Mo, W), which is neutralized by precipitation reaction with Pb^{2+} ions;

In addition, the electrode takes rapidly a stable potential. In the vicinity of the equivalence point, the concentration of MO_4^{2-} ions is low. The second part corresponds to the sudden increase of potential;
Lastly, beyond the equivalent point, we have a significant quantity of Pb^{2+}.

The use of potentiometric titration curves Figures 11 and 12 has given the results summarized in Tableau 5.

Conductimetric dosage
Conductimetric dosage curves E (mV) = f (V_{Pb2+}) (Figures 13 and 14) of tungstate and molybdenum solutions show that the variable measured (conductance) is a linear function of the concentration of ions into solution. The titration curves of the two branches are formed of lines that intersect at the equivalent point. At the beginning of the dosage, the majority of MO_4^{2-} ions in solution are neutralized by the precipitation reaction with Pb^{2+} ions. During the dosage, since the MO_4^{2-} ions are being neutralized, the conductivity of the solution decreases.

Beyond the equivalence point, the conductivity increases. The use of the various conductimetric titration curves has given the results entered in Table 5.

Results of electrochemical characterization (potentiometric and conductimetric) show that B type powders are stoichiometry. These results are in good agreement with those obtained using the gravimetric method. Results obtained by gravimetry, potentiometry and conductimetry show that B type polycrystalline powders are very close to stoichiometry with an average ratio of (Se / Mo ≈ 2.022 and Se / W ≈ 2.056).

Analysis of A type powders
Analyzes conducted on A type powders show that conductimetric and potentiometric dosage curves obtained are similar to those of B type powders. The use of conductimetric dosage curves gave the results entered in Table 6.

459

These results are coherent with those obtained using the gravimetric method and show that Se/Mo ratios in A type polycry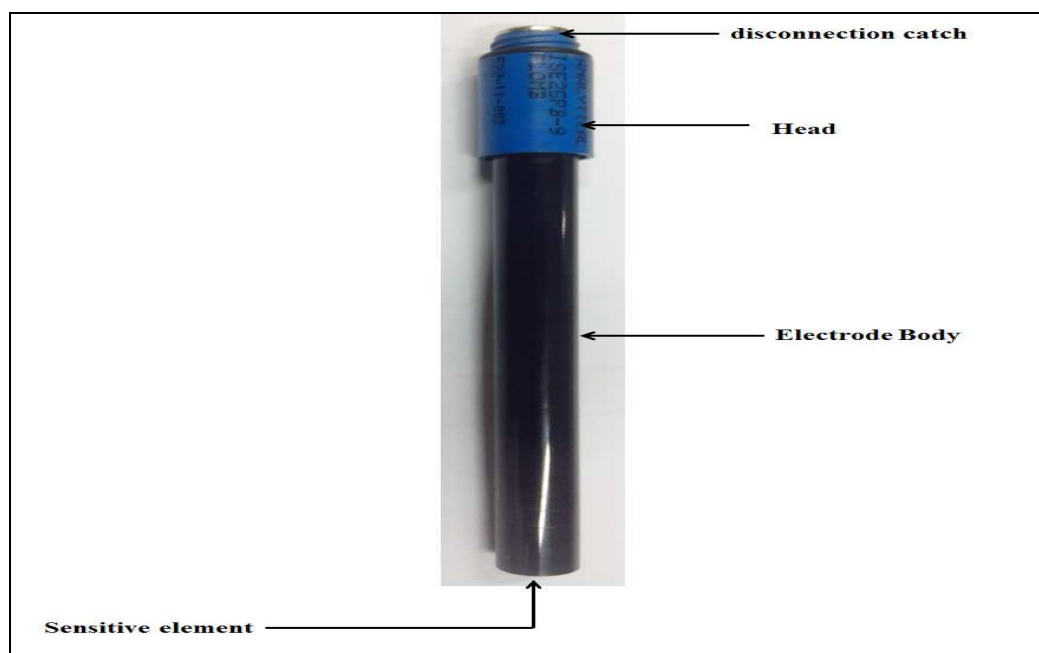stalline powders deviate from the stoichiometry with an average ratio Se/Mo ≈ 1.873 in the approximate range of $1.85 \leq \dfrac{Se}{Mo} \leq 1.9$.
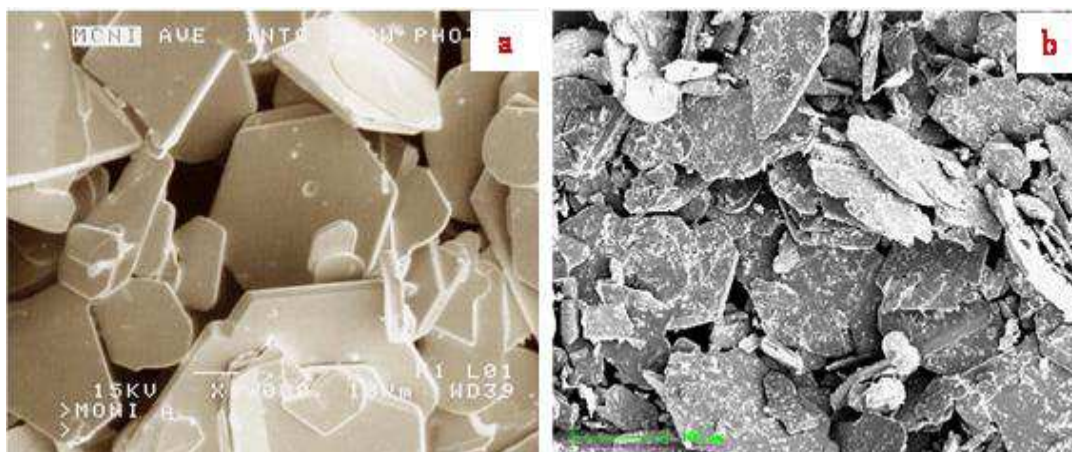

Figure 1: Vacuum pump.
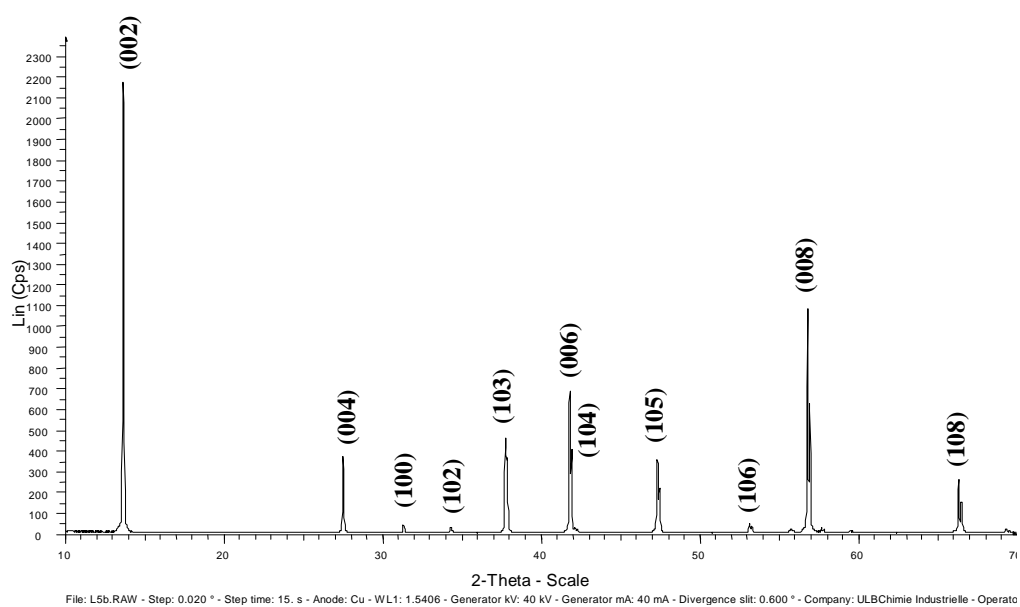

Figure 2: Synthesis Furnace.

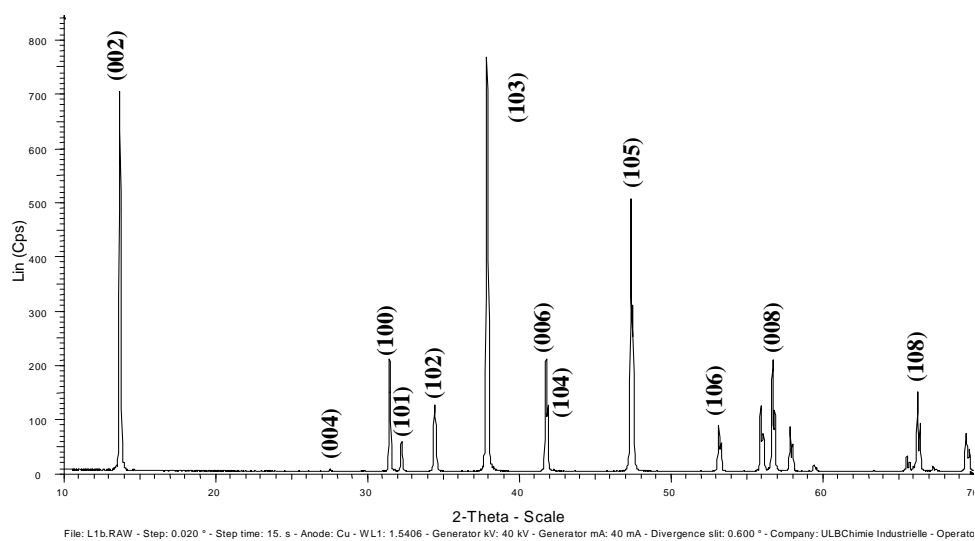**Figure 3:** Selective electrode for ions plomb.

Figure 4: Scanning electron micrographs of molybdenum diselenide. (a): A type molybdenum diselenide polycrystalline powder (13 mm = 20 μm) and (b): B type molybdenum diselenide polyscristalline powder (6 mm = 10 μm).
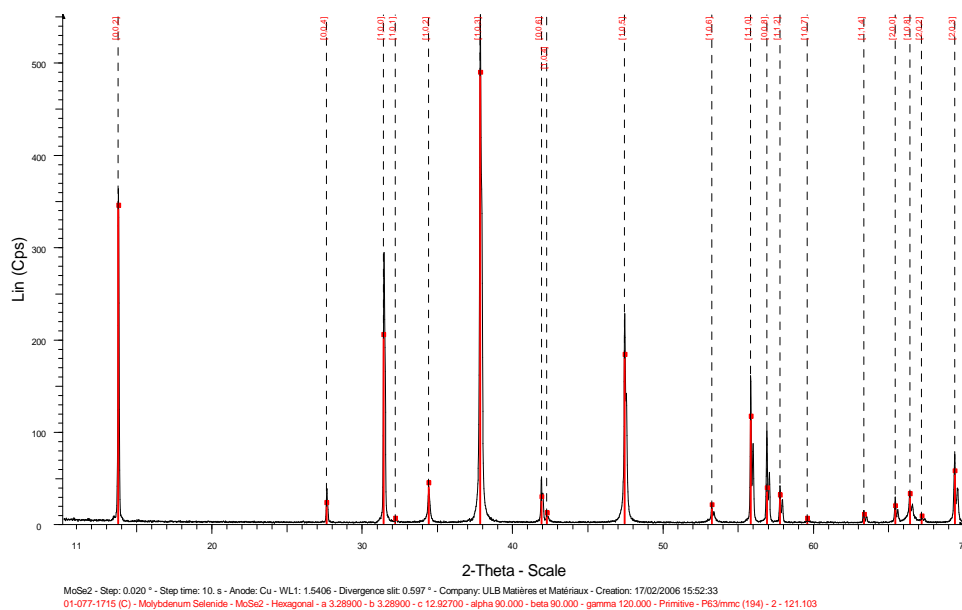
461

Figure 5: Scanning electron micrographs of tungsten diselenide: (a): A type tungsten diselenide polycrystalline powder (13 mm = 20 μm) and (b): B type tungsten diselenide polyscristalline powder (6 mm = 10 μm).

File: L5b.RAW - Step: 0.020 ° - Step time: 15. s - Anode: Cu - W L1: 1.5406 - Generator kV: 40 kV - Generator mA: 40 mA - Divergence slit: 0.600 ° - Company: ULBChimie Industrielle - Operato
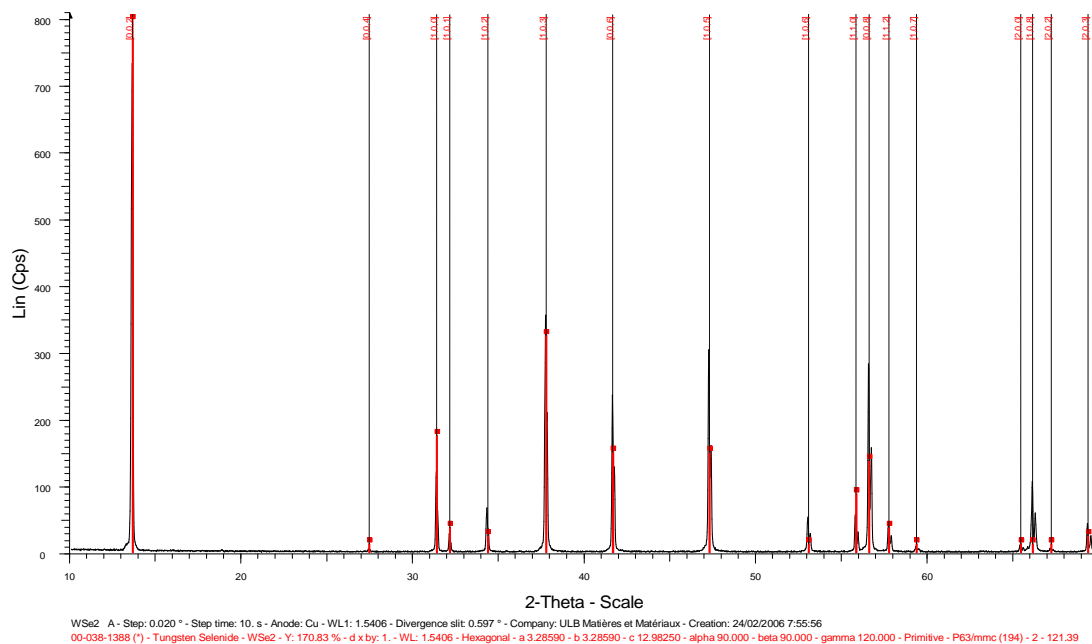
Figure 6 : X-ray diffraction patterns of B type molybdenum diselenide polycristalline powder.
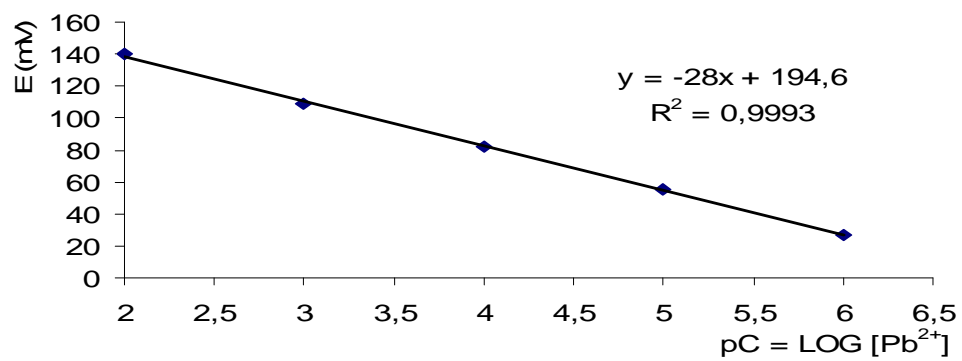
Figure 7 : X-ray diffraction patterns of B type tungsten diselenide polycristalline powder.
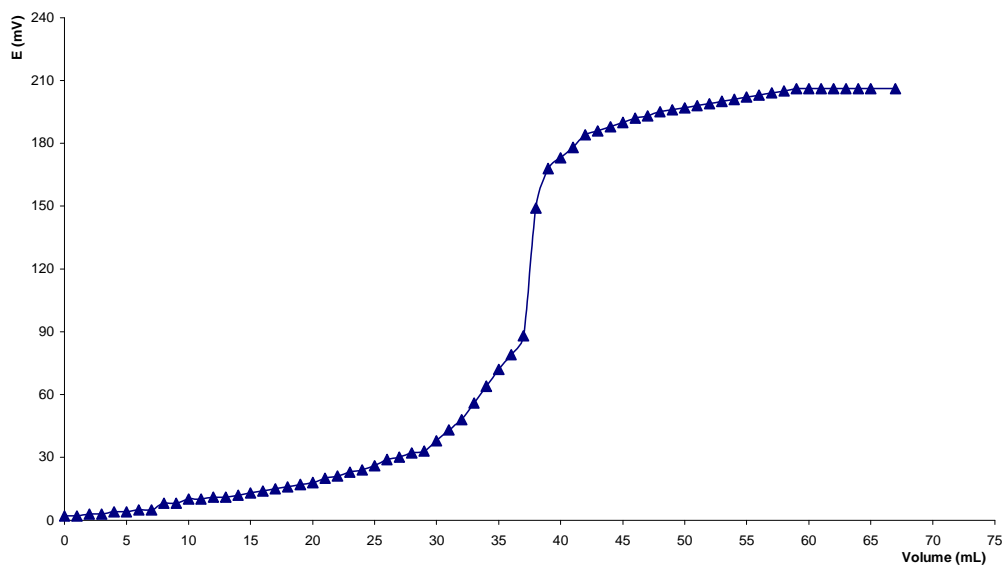

**Figure 8** : X-ray diffraction patterns of A type molybdenum diselenide polycristalline powder.

Figure 9 : X-ray diffraction patterns of A type tungsten diselenide polycristalline powder.
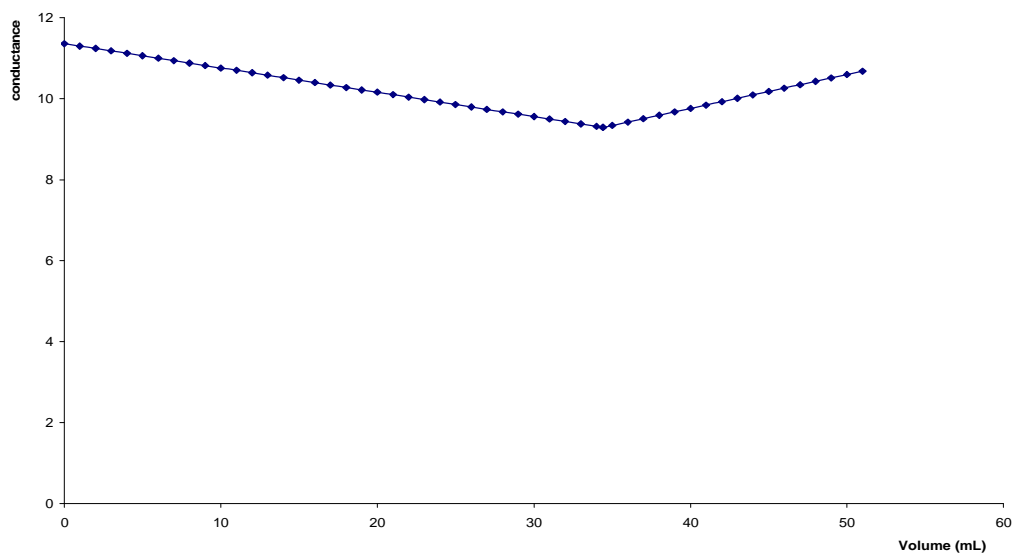

Figure 10: Calibrating curve of the plomb selective electrode.

Figure 11: Potentiometric dosage curve of molybdates ions of MoO_3 dissolving solution using Pb^{2+} using the supporting electrolyte KNO_3 0.1 M.
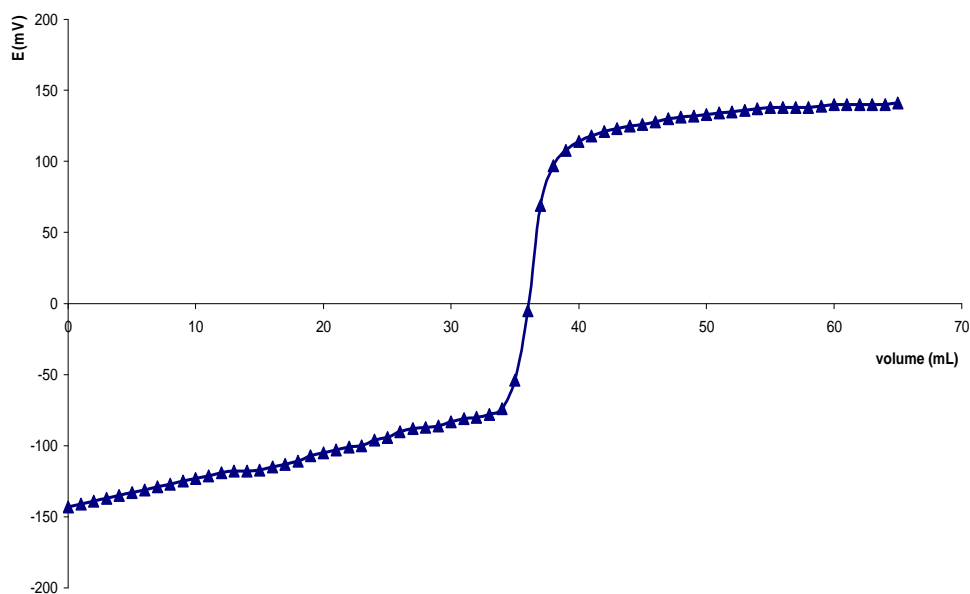
Figure 12: Potentiometric dosage curve of tungstates ions of a dissolution solution of WO_3 by Pb^{2+} using the supporting electrolyte KNO_3 0.1 M.

Figure 13: Conductimetric dosage curve of molybdates ions of a dissolution solution of MoO_3 by Pb^{2+} using the supporting electrolyte KNO_3 0.1 M.
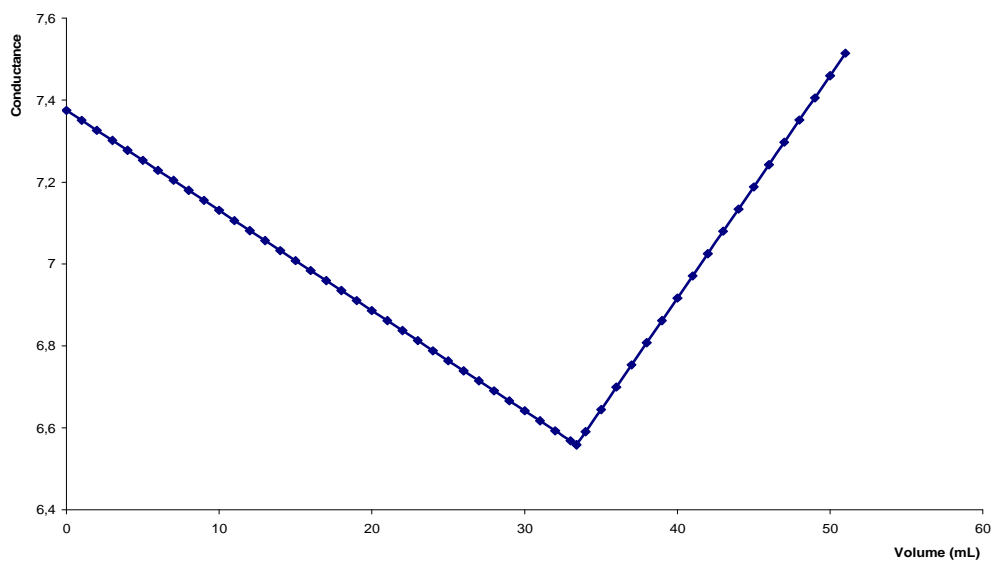
Figure 14: Conductimetric dosage curve of tungstates ions of a dissolution solution of MoO_3 by Pb^{2+} using the supporting electrolyte KNO_3 0.1 M.

Tableau 1a : Results of the use of $MoSe_2$ X-Ray spectra.

hkl	d (hkl)$_A$ (Å)	d (hkl)$_B$ (Å)	d$_{hkl}$ (theoretical) (Å)	δ_A^*	δ_B°
			$MoSe_2$		
002	6.46778	6.46830	6.46500	$2.78\ 10^{-3}$	$3.3\ 10^{-3}$
004	3.23389	3.23415	3.23250	$1.39\ 10^{-3}$	$1.65 10^{-3}$
100	2.85019	2.84995	2.84749	$2.7\ 10^{-3}$	$2.46\ 10^{-3}$
101	2.78343	2.78321	2.78086	$2.57\ 10^{-3}$	$2.35\ 10^{-3}$
102	2.60817	2.60802	2.60592	$2.25\ 10^{-3}$	$2.1\ 10^{-3}$
103	2.37769	2.37761	2.37581	$1.88\ 10^{-3}$	$1.8\ 10^{-3}$
006	2.15593	2.15610	2.15500	$9.3\ 10^{-4}$	$1.1\ 10^{-3}$
104	2.13824	2.13822	2.13670	$1.54\ 10^{-3}$	$1.52\ 10^{-3}$
105	1.91564	1.91565	1.91436	$1.23\ 10^{-3}$	$1.29\ 10^{-3}$
106	1.71943	1.71947	1.71837	$1.06\ 10^{-3}$	$1.1\ 10^{-3}$
110	1.64556	1.64542	1.64400	$1.56\ 10^{-3}$	$1.42\ 10^{-3}$
008	1.61695	1.61708	1.61625	$7\ 10^{-4}$	$8.3\ 10^{-4}$
112	1.59475	1.59463	1.59329	$1.46\ 10^{-3}$	$1.34\ 10^{-3}$
107	1.55056	1.55060	1.54965	$9.1\ 10^{-4}$	$9.5\ 10^{-4}$
114	1.46661	1.46653	1.46537	$1.24\ 10^{-3}$	$1.16\ 10^{-3}$
200	1.42510	1.42498	1.42375	$1.35\ 10^{-3}$	$1.23\ 10^{-3}$
108	1.40639	1.40645	1.40561	$7.8\ 10^{-4}$	$8.4\ 10^{-4}$
202	1.39171	1.39161	1.39043	$1.28\ 10^{-3}$	$1.18\ 10^{-3}$
203	1.35311	1.35285	1.35189	$1.26\ 10^{-3}$	$9.6\ 10^{-4}$

Tableau 1b: Results of the use of WSe_2 X-Ray spectra.

Hkl	d$_{(hkl)A}$ (Å)	d$_{(hkl)B}$ (Å)	d$_{hkl}$(theoretical) (Å)	δ_A^*	δ_B°
			WSe_2		
002	6.49112	6.4900	6.49428	$3.16\ 10^{-3}$	$4.28 10^{-3}$
004	3.24556	3.2450	3.24511	$4.5\ 10^{-4}$	$1.1\ 10^{-3}$
100	2.83673	2.8457	2.84575	$9.02\ 10^{-3}$	$5\ 10^{-5}$
101	2.78069	2.7797	2.77989	$8\ 10^{-4}$	$1.9\ 10^{-4}$
102	2.60706	2.6063	2.60434	$2.72\ 10^{-3}$	$1.96\ 10^{-3}$
103	2.37829	2.3776	2.37777	$5.2\ 10^{-4}$	$1.7\ 10^{-4}$
006	2.16371	2.1633	2.16388	$1.7\ 10^{-4}$	$5.8\ 10^{-4}$
105	1.91837	1.9179	1.91783	$5.4\ 10^{-4}$	$7\ 10^{-5}$
106	1.72261	1.71975	1.72226	$3.5\ 10^{-5}$	$2.51\ 10^{-3}$
110	1.64357	1.64097	1.64345	$1.2\ 10^{-4}$	$2.48\ 10^{-3}$
008	1.62272	1.62076	1.62291	$1.9\ 10^{-4}$	$2.15\ 10^{-3}$
112	1.59329	1.59115	1.59311	$1.8\ 10^{-4}$	$1.96\ 10^{-3}$
107	1.55393	1.55211	1.55374	$1.9\ 10^{-4}$	$1.6\ 10^{-3}$
200	1.42338	1.42154	1.42239	$9.9\ 10^{-4}$	$8.5\ 10^{-4}$
108	1.40981	1.40862	1.41020	$3.9\ 10^{-4}$	$1.58 10^{-3}$
202	1.39034	1.38872	1.39015	$1.9\ 10^{-4}$	$1.43\ 10^{-3}$
203	1.35211	1.35060	1.35173	$3.8\ 10^{-4}$	$1.13\ 10^{-3}$

WSe_2 = diselenide of tungsten, hkl = Miller indexes, d$_{(hkl)A}$ = reticular distances calculated based on experimental results using BRAGG formula: $\lambda = 2\ d_{hkl}\ \sin\theta$ (A type powder), d$_{(hkl)B}$ = reticular distances calculated based on experimental results using BRAGG formula: $\lambda = 2\ d_{hkl}\ \sin\theta$ (B type powder), d$_{hkl}$ (theoretical) **:** reticular distances given by Power Diffraction File (P.D.F), δ_A^* : Gap between d$_A$ and d$_{hkl}$ (theoretical), δ_B° : Gap between d$_B$ and d$_{hkl}$ (theoretical).

Table 2a: Lattice parameters for WSe_2 powders.

Polycrystalline Powders	Parameters		
	a (Å)	c (Å)	c/a
WSe_2 B	3.28647	12.98170	3.95004
WSe_2 A	3.28712	12.98448	3.95010
WSe_2 (theoretical)	3.28600	12.98000	3.95009

WSe_2 = diselenide of tungsten. Lattice parameters are given with an experimental error of ± 0.0001 Å. A This work; A = A type powder; B = B type powder.

Table 2b: Lattice parameters for $MoSe_2$ powders.

Polycrystalline Powders	Parameters		
	a (Å)	c (Å)	c/a
$MoSe_2$ B	3.29060	12.93699	3.9315
$MoSe_2$ A	3.29059	12.93525	3.93098
$MoSe_2$ (theoretical)	3.28900	12.92700	3.93037

$MoSe_2$ = diselenide of Molybdenum. Lattice parameters are given with an experimental error of ± 0.0001 Å. A This work; A = A type powder; B = B type powder.

Table 3: Results of the gravimetric analysis.

Polycrystalline Powders	$\frac{Se}{M}$ Ratio A type powders	$\frac{Se}{M}$ Ratio B type powders	Theoretical $\frac{Se}{M}$ ratio
$MoSe_2$	1.8857	2.0255	2
WSe_2	1.9148	2.0255	2

$MoSe_2$ = diselenide of molybdenum, WSe_2 = diselenide de tungsten. Each Se/M ratio is given with an error of ± 0.0003. The Se/M ratio has been calculated from experimental gravimetric measurements, using an electronic analytical balance (Δm = 0.0001 g).

Table 4: Results of the calibrating selective electrode for ions plomb.

Measure N°	$[Pb^{2+}]$ (mol/ℓ)	pC = -Log $[Pb^{2+}]$	Potential (mV)	Response Time (s)	Temperature (°C)
1	10^{-6}	6	27	93	29,7
2	10^{-5}	5	55	70	29,9
3	10^{-4}	4	82	64	30
4	10^{-3}	3	109	53	30
5	10^{-2}	2	140	42	30

Pb = Plomb, detection limit = 3. 41 10^{-7} mol/l, slope = 99. 93 %, potential stability criterlium = 0.15 mV/ min.

Table 5: Results of the potentiometric and conductimetric dosage of B type powders.

	Polycrystalline powders Synthetized in laboratory	Quantity of initial powder (g)	Mass of metal obtained (g)	Ratio $\frac{Se}{M}$ of various powders	Theoretic al ration
Potentiometry	MoSe$_2$	3.2596	0.8994	2.021	2
	WSe$_2$	3.2596	1.7236	2.049	2
Conductimetry	MoSe$_2$	3.2596	0.8970	2.020	2
	WSe$_2$	3.2596	1.7189	2.086	2

MoSe$_2$ = diselenide of molybdenum, WSe$_2$ = diselenide of tungsten. Each Se/M ratio is given with an error of ± 0.0003. The Se/M ratio has been calculated from experimental conductimetric and potentiometric measurements, using an electronic analytical balance (Δm = 0.0001 g).

Table 6: Results of conductimetric dosage of A type powder.

Polycrystalline Powders	Quantity of initial powder (g)	Mass of metal obtained (g)	$\frac{Se}{M}$ Ratio	Theoretical ratio
MoSe$_2$	3.2596	0.9461	1.861	2
WSe$_2$	3.2596	1.7865	1.920	2

MoSe$_2$ = diselenide of molybdenum, WSe$_2$ = diselenide of tungsten. Each Se/M ratio is given with an error of ± 0.0003. The Se/M ratio has been calculated from experimental concuctimetric measurements, using an electronic analytical balance (Δm = 0.0001 g).

DISCUSSION

In literature, three phases are known in case of a Mo-Se system: Mo_3Se_4, $MoSe_2$, $MoSe_3$. But currently, only two polytypes are known: 2Hb and 3R (Kuc et al., 2011; Sundaram et al., 2013). Polytypes are identical to those known for MoS_2 where a 2Hb mesh contains two layers Se-Mo-Se whereas the mesh 3R contains three layers Se-Mo-Se. Works by Deshplande et al. (1999 and Liu et al. (2011) highlighted the influence of the composition in M_o and Se on the structure observed for $MoSe_2$. Two composition ranges were observed according to the value of the Se/M_o ratio. For $1.9 \leq \frac{Se}{Mo} \leq 2.0$ composition, the spectra give peaks of thin diffractions and are characterized by a preferential orientation of the reflection planes (00ℓ). This is quite different in composition $1.85 \leq \frac{Se}{Mo} \leq 1.9$. For this composition,

there is no any preferred orientation of the peaks (00ℓ). Furthermore, lines (103) and (105) have a wider basis than the other lines. This broadening at the basis of lines (103), (105) would be due to a mixed piling of 2Hb and 3R layers (Karunadasa et al., 2012; Jonathan et al., 2014). Our experimental results are consistent with these observations.

Powders $MoSe_2$ B with a $\frac{Se}{M_o}$ ratio close to 2 are well characterized by a diffraction spectrum of the same type as that described by Naruke et al. However, A type powders, with a $\frac{Se}{M_o}$ ratio of 1.88, are well characterized by a diffraction spectrum identical to that described in literature for the composition $1.85 \leq \frac{Se}{Mo} \leq 2.0$. It can therefore be

considered for this type of powder, a mixed piling of layers 2Hb and 3R. However, the development of 3R layers does not have any impacts on the conduction properties of these materials due to the fact that the electronic structures of 2Hb and 3R are identical. The parameters of the mesh given in Tables 1a and 1b do not show any difference between both types of powders. Differences are mainly noticed at the morphological level as noticed in the results obtained using the scanning electron microscopy. For the W-Se system, only one phase is known, i.e. WSe_2. Only 2Hb polytype is known, the rhombohedral polytype has not been identified (Pourbaix, 1963; Boubié et al., 2008). The value of the Se/W ratio seems to have no influence on the structural characteristics of both A and B types of powders: all the diffraction peaks are fine with no particular preferred orientation (Deshpande et al., 1999).

Conclusion

Polycrystalline molybdenum and tungsten ($MoSe_2$, WSe_2) diselenides were synthesized at 1323 K for 168 hours in silica tubes sealed secondary vacuum. The work is mainly a contribution to determine the structure, morphology and stoichiometry of polycrystalline powders ($MoSe_2$ and WSe_2). The variation in synthesis conditions of polycrystalline powders enabled to produce two types of powders:

➤ B type Powder obtained by air quenching ;

➤ A type Powder obtained by cooling the synthesis tube within the furnace over half a day.

It has been also shown that synthesis conditions have also an impact on the stoichiometry of our materials and their morphology. Although mesh parameters are identical regardless of the method used to make the synthesis, results have shown that stoichiometry is reached only when using B type powders and a difference in layer piling according to the mode of synthesis; this explains why A type powders differ from B type powders due to the piling of 2H: 3R layers.

REFERENCES

Boubié G, Tiriana S, Legma JB, Delplancke MP Ogletree. 2008. Caractérisation Structurale de Diséléniures de Molybdène et de Tungstène dopés au Rhénium. *J. Soc. Ouest-Afr. Chim.,* **25**: 71 – 85.

Bougouma M, Boubié G, Tiriana S, Legma JB, Delplancke MP Ogletree. 2008. The Structure of Niobium-Dopés $MoSe_2$ and WSe_2. *Bull. Chem. Soc. Ethiop.,* **22**(2): 225-236.

Deshpande MP, Patel PD, Vashi MN, Agarwal MK.1999. Effect of intercalating indium in WSe_2 single Crystals. *J. Crystal Growth,* **197**: 833-840.

Forker M, SchmidtbergerJ, Szabó DV, Vollath D. 2000. Perturbed- Angular- Correlation Study of Phase Transformations in Nanoscaled Al_2O_3 - coated and Uncoated ZrO_2 Particles Synthesized in a Microwave Plasma. *Phys. Rev.,* **B61**: 1014-1025.

Huang X, Zeng ZY, Zhang H. 2013. Metal dichalcogenide nanosheets: preparation, properties and applications. *Chem. Soc. Rev*., **42**: 1934 -1946.

JCPDS X-ray Powder Data file, Pattern: 01-077-1715.

JCPDS X-ray Powder Data file, Pattern: 01-087-2418.

Jonathan CS, Hailong Z, Yu C, Nathan OW, Yuan L, Yu H, Xiangfeng D. 2014. Chemical vapor deposition growth of monolayer $MoSe_2$ nanosheets, *Nano Research.* DOI 10.1007/s12274‐014‐0147‐z.

Karunadasa HI, Montalvo E, Sun YJ, Majda M, Long JR, Chang CJ. 2012. A Molecular MoS_2 edge site mimic for catalytic hydrogen generation. *Science,* **335**: 698‐702.

Kuc A, Zibouche N, Heine T. 2011. Influence of quantum confinement on the electornic structure of the transition metal sulfide TS_2. *Physical Review*, **B 83**: 245213.

Li Y, Wang HL, Xie LM, Liang Y, Hong GS, Dai HJ. 2011. MoS$_2$ nanoparticles grown on graphene: an advanced catalyst for the hydrogen evolution reaction. *J. Am. Chem. Soc.,* **133**: 7296‑7299.

Liu L, Kumar SB, Ouyang Y, Guo J. 2011. Performance limits of monolayer transition metal dichalcogenide transistiors. IEEE Trans. *Electron Devices*, **58**: 3042‑3047.

Perkins FK, Friedman AL, Cobas E, Campbell PM, Jernigan GG, Jonker BT. 2013. Chemical vapor sensing with monolayer MoS2. *Nano Lett.,* **13**: 668‑673.

Pourbaix M. 1963. *Atlas d'Equilibre Electrochimiques à 25 °C.* G. Gauthier Villard et Cie éditeurs : Paris.

Radisavljevic B, Radenovic A, Brivio J, Giacometti V, Kis A. 2011. Single‑layer MoS2 transistors. *Nat. Nanotech.,* **6**: 147‑150.

Sortais-Soulard C. 2004. Equilibres oxydo-réducteurs dans les MQ2 (M = Pt, Pd; Q = Se,Te) - Influence de la pression sur la redistribution du nuage électronique, Thèse de doctorat, Université de Nantes, Nantes, p.105.

Sundaram RS, Engel M, Lombardo A, Krupke R, Ferrari AC, Avouris Ph, Steiner M. 2013. Electroluminescence in single‑layer MoS2. *Nano Lett.,* **13**: 1416‑1421.

Vollath D, Szabó DV. 2006. The microwave plasma process – a versatile process to synthesize nanoparticulate materials. *J. Nanoparticle Research*, **8**: 417- 428.

Zhu CF, Zeng ZY, Li H, Li F, Fan CH, Zhang H. 2013. Single‑layer MoS2‑based nanoprobes for homogeneous detection of biomolecules. *J. Am. Chem. Soc.,* **135**: 5998‑6001.